Recent Research in Genetics and Genomics 2019; 1(1): 29-47

Original article:

Accumulative persistence of the genotoxic and mutagenic effects induced by low doses of TiO_2 nanoparticles increases the incidence of hepatocellular carcinoma in mice

"TiO2 nanoparticles and hepatocellular carcinoma"

Hanan R. H Mohamed[1*], Andrew Tharwat[2], Sara Edwar[2], Lidia Samir[2], Engy Salah[2] and Omar Tarek[2]

[1:] Zoology Department; [2:] Biotechnology/Biomolecular program; Faculty of science Cairo University; Giza, Egypt. [*:] Correspondence to: hananesresm@yahoo.com

doi: 10.21608/RRGG.2019.56175. Received: 14 October 2019; accepted: 27 October; published 01 November 2019

Abstract

Nowadays, titanium dioxide nanoparticles (TiO_2NPs) are widely used in toothpaste, sweets, food perseveration, chewing gum and medicine. Therefore, humans are exposed to large amounts of this substance in their daily lives. However, limited studies are available on the persistence of TiO_2NP-induced genotoxicity and mutagenicity in liver tissues. Therefore, this study was designed to investigate the persistence of TiO_2NPs-induced genotoxicity and mutagenicity and possible hepatocellular carcinoma induction in mice. The oral administration of TiO_2NPs at the two dose levels 5 and 50 mg/kg b.w caused persistent DNA breaks and apoptotic DNA damage, as well as concurrent persistent high mutation induction was observed in both the exons 5 & 8 of p53 gene and exons 1&2 of H-ras gene of mice administered TiO_2NPs during the experimental time in direct proportional to the sampling time. Moreover, histological examinations revealed necrosis of the liver tissue during the experimental period. This damage could be attributed to the persisted significant increases in the malondialdehyde level and reduction in the antioxidant glutathione level demonstrated in TiO_2NPs groups. In conclusion, oral administration of even the low safe dose of TiO_2NPs resulted in persistent DNA damage, apoptosis, and oxidative stress that ultimately lead to necrosis in the entire liver architecture and thus increases the incidence of hepatocellular carcinoma.

Keywords: DNA damage; TiO_2 nanoparticles; p53 gene; H-ras gene; hepatocellular carcinaoma; oxidative stress and mice

1-Introduction

Nowadays, there is a growing interest worldwide in using the engineered nanoparticles (ENPs) in our daily life due to their wide applicable properties that suit many sectors as industry, medicine, and material science that raising serious concerns about its potential danger to human health **(Mohamed, 2015)**. Moreover, nanoparticles can enter circulation accumulating in various organs as lungs, spleen, bone marrow and liver tissues, this accumulation contributes in introducing and developing many nanoparticle associated diseases in various systems as cardiovascular and respiratory diseases which can lead to cellular carcinoma **(Mohamed, 2015; Smulders *et el*, 2014)**.

The vast uses of ENPs are in paints, food, medicine and coating industries. As the three major used ENPs are silver, silicon dioxide, and titanium nanoparticles, in Europe TiO2 ENPs alone comprise 25% of the total ENPs usage in this sector (Smulders *et el*, 2014). In our research, we will focus on Titanium dioxide (TiO_2) nanoparticles (NPs) due to its remarkable properties such as its high optical performance, high redox activity, high stability, anticorrosive, good photo catalytic activity, the large surface area which also increase the risk of toxic human exposure.

TiO_2 NPs are widely used in the industry of the common household products as paints, plastics, and electronics in addition to their uses in various cosmetics such as face creams, sun block creams and toothpaste due to its high stability and anticorrosive properties. They are also used in food additives such as candies, sweets, gums, and artificial flavors **(Weir *et al.*, 2012; Mohamed, 2015; Smulders *et el*, 2014).** In medicine TiO_2 NPs are is used in cancer Therapy as they are it is considered as a potential photo-synthesizers for photodynamic therapy by absorbing near IR light and also the photo-activated TiO_2 NPs exhibit selective cytotoxicity against breast epithelial cancer cells, it also shows a fatal impact on some viruses such as hepatitis C, poliovirus 1, and herpes simplex virus **(Weir *et al.*, 2012)**.

However, exposure to TiO_2 NPs has a toxic effect on human health as they can interact with internal cell organelles leading to structural and functional modifications. Recent evidences shows that TiO_2 NPs induce neurotoxicity, nephrotoxicity and can also affect bone cell viability, proliferation, and differentiation **(Long *et al.*, 2007; Jeon *et al.*, 2011; Masoud *et al*, 2015)**.

Moreover, nano-TiO_2 clastogenicity and genotoxicity have been evidenced by the assessed chromosomal and DNA breaks induction using micronucleus and comet assays both in *in vitro* e.g. L5178Y mouse lymphoma cells, Syrian hamster embryo cells and in human bronchial epithelial cell line **(Nakagawa *et al.*, 1997; Gurr et al., 2005; Guichard *et al.*, 2012)** and in *in vivo* e.g. in mouse

peripheral blood and in earthworm (Trouiller et al., 2009; Hu et al., 2010). Toxic effect of TiO_2 NPs can be clearly examined by observing the generation of the reactive oxygen species (ROS) and their oxidative stress. The response to increased ROS generation has been reported to introduce a series of pathological effects as genotoxicity, carcinogenicity, and neurotoxicity **(Long *et al*., 2007)**.

The interaction between TiO_2 NPs and macromolecules also leads to various deleterious process resulting in an imbalance between ROS generation and antioxidant defenses that subsequently increased the ROS generation leading to cellular apoptosis, DNA lesions which introduce the incidence of cancer in liver tissue, considering the liver the body first organ to fight TiO2 NPs toxicity and have a high content of antioxidant defenses, especially in our research which focused on the oral route of TiO_2 NPs exposure **(Turrens, 2003)**.

The wide uses of TiO_2 NPs in toothpaste and as food colorants and nutritional supplements make the oral exposure as a basic route for their exposure. And due to limited research on bio-persistence of nano-TiO_2 induced genotoxicity and mutagenicity in liver tissues, in our research we evaluated the impact of the bio-persistence of nano-TiO2 induced genotoxicity, mutagenicity on the incidence of cancer in liver tissue following the oral exposure of Nano-TiO2 particles.

Comet and DNA laddered fragmentation assays were done to assess DNA breaks and apoptosis while single strand conformational polymorphism (SSCP) analysis was carried out to screen mutation in the p53 gene (exons 5 & 8) and H-ras exons (1 & 2). Histopathological examinations of liver tissues and biochemical measurements of oxidative stress markers including malondialdehyde (an indicator of lipid peroxidation) and reduced glutathione (antioxidant protein) were done to shed more light on the mechanism of nano-TiO_2 induced toxicity.

2-Materials & Methods

2.1Animals

Male Swiss Webster mice weighting 25–28 gm were obtained from the animal house of National Organization for Drug Control and Research (NODCAR). They were left in the lab for one week under standard dark/light cycle to be acclimatized with the laboratory conditions and supplied with standard diet pellets and water that were given ad libitum.

2.2 Chemicals

All used chemicals were purchased from sigma Company. TiO_2 nanoparticles <100nm were purchased in the form of white powder (Sigma chemical Co., St. Louis, MO) and suspended in deionized distilled water to prepare the tested desired doses (5&50 mg/kg b.w).

2.3 Characterization of Nano TiO2 for Injection

2.3.1 X-Ray Diffraction

The X-ray diffraction (XRD) patterns of nano-TiO_2 particles were measured according to the routine work using a charge coupled device diffractometer (XPERT-PRO, PANalytical, The Netherlands). Particle size was calculated using the Scherrer's relationship (D = 0.9 k/Bcosh), where k is the wavelength of X ray, B is the broadening of diffraction line measured as the half of its maximum intensity in radians, and h is the Bragg's diffraction angle. The particle size of the sample has been estimated from the line width of XRD peak.

2.3.2 Transmission Electron Spectroscopy (TEM)

TiO_2 nanoparticles suspensions in Milli-Q water were sonicated at 40 W for 20 min, then drop of TiO_2 suspensions were coated on carbon-coated copper transmission electron spectroscopy (TEM) grids, dried, and finally TEM (a TecnaiG20, Super twin, double tilt) was operated at an accelerating voltage of 200 kV to image nano-TiO2 particles and detect their morphology and particle average size.

2.4 Treatment schedule:

All animals were housed and treated in accordance with the Guidelines of the National Institute of Health (NIH) regarding the care and use of animals for experimental procedures. Forty-five animals were divided randomly into four groups. The first two groups are negative (deionized dist. H2O) and positive (CCl4 at the dose 1ml/kg (3 olive oil: 1 CCL4)) control groups, while both the third and fourth groups were orally administered TiO_2 nanoparticles at the two different dose levels 5 and 50 mg/kg. b.w for five consecutive days and sacrificed after 24 h, 1 week and 2 weeks of the last treatment.

2.5 Alkaline Comet assay

To detect genotoxicity in virtually any mammalian cell type without requirement for cell culture. The alkaline (pH >13) comet assay was performed according to **Tice *et al.*, (2000)** as following: glass Slides were scratched to ensure the fixation of gel on it. Then immersed in 1% Agarose gel and left overnight to cool down. A low melting point agarose gel was applied on the pre-homogenized sample of DNA from 28 samples and mixed gently. Then 80µl of the sample was taken and applied on the slide and stretched out on the slide. After incubation in the alkaline buffer, all slides was applied in electrophoresis for 20 min. at 300 mA and 25 V. finally, fixed in 100% cold ethanol, air dried and stored at room temperature until they were examined.

2.6 Ladder DNA fragmentation assay

This assay was done to assess apoptotic DNA fragmentation using suitable DNA extraction kit in briefly: grinded up 20 mg of liver tissues and re-suspended in 180µl of digestion solution. Then added 20µl of proteinase K solution and 200µl of lysis solution mixed thoroughly by vortex and incubated at 56oc for complete denaturation and

solubilization of proteins. Finally added 400µl of 50% ethanol and mix by pipetting for DNA precipitation, Centrifuge the column for 1 min at 6000x g and then wash using washing buffer I and II. Finally, added 200µl of elution buffer to elute DNA in the micro-centrifuge tube. The purified DNA was separated by electrophoresis in 2% agarose gel at 70 V and visualized using a UV trans-illuminator and photographed.

Table 1: Sequences of primers used for amplification of *p53 and H-ras* Genes

Gene	Exons	Stand	Sequence
P53	5	Sense	TACTCTCCTCCCCTCAATAAG
		Antisense	ACCATCGGAGCAGCCCTCA
	8	Sense	GGGAACCTTCTGGGACGGGAC
		Antisense	TCTCTTTGCGTCCCCTGGGGG
H-Ras	1	Sense	ACAGAATACAAGCTTDTGGTGGTG
		Antisense	CTCTATAGTGGGATCATACTCGTC
	2	Sense	GACTCCTACCGGAAACAGGTGTC
		Antisense	GGCAAATACACAGAGGAAGCCCTC

2.7 SSCP analysis

Polymerase chain reaction (PCR)-based SSCP was used to screen for the presence of mutations in p53 (exons 5 & 8) and H-Ras (exons 1 &2).

2.7.1 Isolation of Genomic DNA

DNA pellet was extracted from liver tissue using Gene JET Genomic DNA Purification kit (Thermo Scientific #K0721, #K0722). After homogenization of 20 mg tissue in a 180 µl digestion buffer, we add 20 µl proteinase k (20 mg/µl) to break down cell membranes and intracellular connective tissue. Put the samples in a shaking incubator for 30 minutes at room temperature. Add 200 µl lysate solutions to the samples for breaking down of all nuclear and cell membranes. Centrifuge the samples at 14000 rpm for 15 minutes at room temperature. Transfer the supernatant to a new tube. An equal volume of 100% cold ethanol was added for precipitation of DNA and finally, centrifuge at 14000 rpm for 20 minutes. DNA pellet was washed with 400 µl of

100% cold ethanol. Pour off the ethanol briefly and keep the tubes open to let the pellet dry. The DNA pellet was washed twice with 70% ethanol dried and finally suspended it in sterile distilled water.

2.7.2 PCR amplification

Amplification of genomic DNA was done for P53 gene (exons 5 & 8) and H-RAS gene (exons 1 & 2) through the succession of incubation steps at different temperature using the previously designed primer sequences shown in Table 1 **(Gutierrez *et al*., 1992; Watanabe *et al*., 1999).** The PCR reaction mixture was set up by mixing 2.5 µl (250 ng) of extracted genomic DNA sample, 1µl (50 pmol), 1 µl (50 pmol) of reverse primer and 5 µl of the master mix then complete PCR volume to 10 µl with dist deionized water. Cycling was started in Thermal Cycler (Programmable Thermal Cycler, PTC-100 thermal cycler, Model 96 (MJ Research, INC., Watertown, MA)), with initial denaturation at 95◦C for 5 min. Thirty cycles of denaturation (95◦C), annealing (58◦C for p53 exons 5 and 8), (60◦C for H-Ras exons 1 and 2), and extension (72◦C) were done. A final extension at 72◦C for 10 min was necessary for complete amplification. PCR products were separated and visualized by electrophoresis through 2% ethidium bromide-treated agarose gel (Sigma, UK) using UV trans-illuminator (Stratagene).

2.7.3 SSCP analysis

After obtaining the amplified samples prepare the Acrylamide gel. But first, prepare the sample by adding 5µl loading dye for each sample and exposing them to heat at 950 C for 7 min. to denature PCR products before loading quickly placed them into ice after removing from heat to prevent annealing of two strands. The denatured PCR samples were subjected to 20% polyacrylamide gel electrophoresis (acrylamide: bisacrylamide = 49:1 v/v). Each gel (8 cm x 7.3 cm x 1 mm) was cast using the Bio-Rad mini-Protean II set. Poly- acrylamide gel (10 ml) was prepared by mixing 4 ml of 50% acrylamide/bisacrylamide mixture, 1-ml 10% TBE buffer, 5-ml sterile double distilled water, 100 µl of 10% ammonium persulfate (freshly prepared), and at the last 10 µl of TEMED (tetram-ethylethylenediamine)inanErlenmeyerflask.

Samples were electrophoresed at 100 V till the dye reached the bottom of the gel (about 45 min), after that gel was stained for 10 min with ethidium bromide to visualize the DNA bands with the aid of shaking. The gel was placed on a UV transilluminator (Stratagene) and a picture of the fluorescent ethidium bromide stained DNA separation pattern was taken with a Polaroid camera (PolaroidMP4 Land Camera).

2.8 Histopathology

It is more specific and shows the necrotic cells and the pathogenicity of the nanoparticles on the tissue level. Portions of liver tissues were fixed in formalin 10% to preserve the cellular structure of the tissue. After fixation, the water must be

removed from the liver tissue block, a process called dehydration. Prior to sectioning, the liver tissue block must be infiltrated with a material that acts as a support during the sectioning process. Sectioning is accomplished by using a cutting apparatus called a microtome and stained with hematoxylin and eosin. The final step in this procedure is to permanently mount the sections under a cover slip. This is accomplished by covering the section in a medium that will harden and produce a clear binder between the slide and cover slip.

2.9 Measurement of biochemical marker of oxidative stress:

A portion of the liver of all groups was homogenized using saline to prepare 10% homogenate, centrifuged to separate cell pellet &debris and obtained the clear supernatant. The Clear supernatant was used to measure reduced glutathione (GSH) & malondialdehyde (MDA) levels. MDA was measured spectrophotometricaly according to the methods described by **Ohkawa et al., (1979).** Thiobarbituric acid (TBA) reacts with malondialdehyde (MDA) in acidic medium at the temperature of 950C for 30 min. to form thiobarbituric acid reactive product and the absorbance of the resultant pink product can be measured at 534nm. On the other hand, the method used for measurement of GSH level was based on the reduction of 5,5dithiobis (2-nitrobenzoic acid)(DTNB) with glutathione (GSH) to produce a yellow compound .the reduced chromogen directly proportional to GSH concentration and its absorbance was measured at 405 nm **(Beutler *et al*., 1963)**.

2.10 Statistical analysis

Results were expressed as Mean ± SD and SPSS analysis software was used to analyze all data and compared between the treated groups, negative and positive control using independent T-test. One way of analysis of variance (ANOVA) was used to test the effect of time on the tested parameters.

3-Results

3.1 TiO2 Nanoparticles Characterization

Results of nano-TiO_2 characterization published in our previous study Mohamed, (2015) evidenced the nano size of TiO_2 particles both in dry and aqueous state. XRD pattern of TiO_2 nanoparticles confirmed the purchased form of rutile and anatase TiO_2 nanoparticles by the peaks that were corresponding with the tetragonal rutile and anatase structure of TiO_2NPs. No impurity phase was observed in the sample. The average crystallite size of the samples was calculated using Debye Scherrer's formula and found to be about 44 nm.

The TiO2 nanoparticles were found to be in the nano scale range in water, but formed small agglomerates in aqueous solution. The average size measured was 45.63 ± 12.85 nm. This was further confirmed by the obtained dynamics laser

scattering (DLS) data that had shown that the nano-TiO_2 particles had a distribution of 20–85 nm (50.46 ± 21.20) in H2O (Mohamed, 2015). The typical TEM image suggests that most of the TiO2-NPs are crystallites with polyhedral morphologies thus increasing its surface area and its activity.

3.2 Comet assay

Results of comet assay are summarized in table 2 as oral administration of nano-titanium (5 and 50 mg/kg) induced high DNA damage inductions as revealed by the statistical significant elevations ($p<0.001$) in tail length, % DNA in tail and tail moment compared with the negative control group and even reached to the DNA damage induced by hepatic injured carbon tetrachloride. Moreover, nao-TiO_2 induced DNA was increased by increasing the sampling time in spite of stopping its administrations as indicated by the high significant difference ($p<0.001$) between different groups treated with the same dose of nano-titanium at different sampling time using analysis of variance evidenced.

3.3 Laddered DNA fragmentation

In agreement with the results of comet assay, qualitative assessment of apoptotic DNA fragmentations evidenced apoptotic DNA damage inductions by orally administrated TiO_2 nanoparticles at the tested doses 5 and 50 mg/kg in a time-dependent manner. This was revealed by the observed dramatic degraded pattern of genomic DNA of nano-titanium treated groups (Fig. 1) indicated by the appearance of both laddered fragmentized and smeared pattern of genomic DNA running on the agarose gel (Fig. 1) compared with undamaged genomic DNA of the negative control group. Moreover, nano-titanium induced DNA damage reached to that induced in the positive control group treated with carbon tetrachloride.

3.4 SSCP analysis

Results of SSCP analysis were summarized in table 3 and representative micrograph for the observed mutations in p53 and H-ras exons in liver cells was shown in Fig. 2a and 2b. In p53 exon 5 no any mutation was observed in mice treated with nano titanium (5 mg/kg) after 24 hours. On contrary two mice out of four and three mice out of five mice treated with 5mg of nano-TiO_2 (group 2) after one and two weeks respectively (Table 3). While mice treated with 50 mg of nano-titanium (in group 3), two mice out of the four (24 hours), two mice out of four (one week) and three out of five (two weeks) mice were mutated as shown in table 3.

On contrary, high mutation incidence was observed in in p53 exon 8 in both groups two (5 mg/kg): two mice out of four (after 24 hour and one week) and three mice out of five mice (after two weeks) as shown in table 3, and in the group three (50 mg/kg): four mice out of four and three mice out of five sacrificed after 24 hour, one week and two weeks, respectively.

Table 2: Tail length, % DNA in tail and tail moment in groups treated with nano-TiO_2 particles and the control groups

Group	Dose	Duration	Tail length (px)	% DNA in tail	Tail moment
Negative Control	_	pooled	7.1±1.0	26.2±2.7	1.8±0.4
Positive Control	1 ml/kg	Pooled	17.2±1.5^{a***}	30.2±2.3^{a*}	5.9±0.9^{a***}
Nano-TiO_2	5 mg/kg	24 h 1 week 2 week	15.3±2.0^{a***} 7.1±1.9^{a***,b*} 30.2±1.8^{a***,b***}	37.2±0.5^{a***,b*} 45.3±1.4^{a***,b***} 51.4±2.7^{a***,b***}	5.9±1.3^{a**} 9.1±0.9^{a***,b**} 15.5±1.4^{a***,b***}
One way ANOVA			F=71 P<0.001	F=62 P<0.001	F=67 P<0.001
Nano-TiO_2	5 mg/kg	24 h 1 week 2 week	28.7±1.2^{a***,b***} 40.2±0.7^{a***,b***} 55.7±3.4^{a***,b***}	43.3±3.1^{a***,b***} 56.6±3.2^{a***,b***} 71.0±3.0^{a***,b***}	12.5±1.4^{a***,b***} 22.7±1.4^{a***,b***} 39.5±2.4^{a***,b***}
One way ANOVA			F= 158 P<0.001	F=87 P<0.001	F=247 P<0.001

Results are expressed as mean ± S.D

[a]: indicated statistically significant difference from the negative control group

[b]: indicated statistically significant difference from the positive control group at [*]: p<0.05, [**] p<0.01 and [***] p<0.001

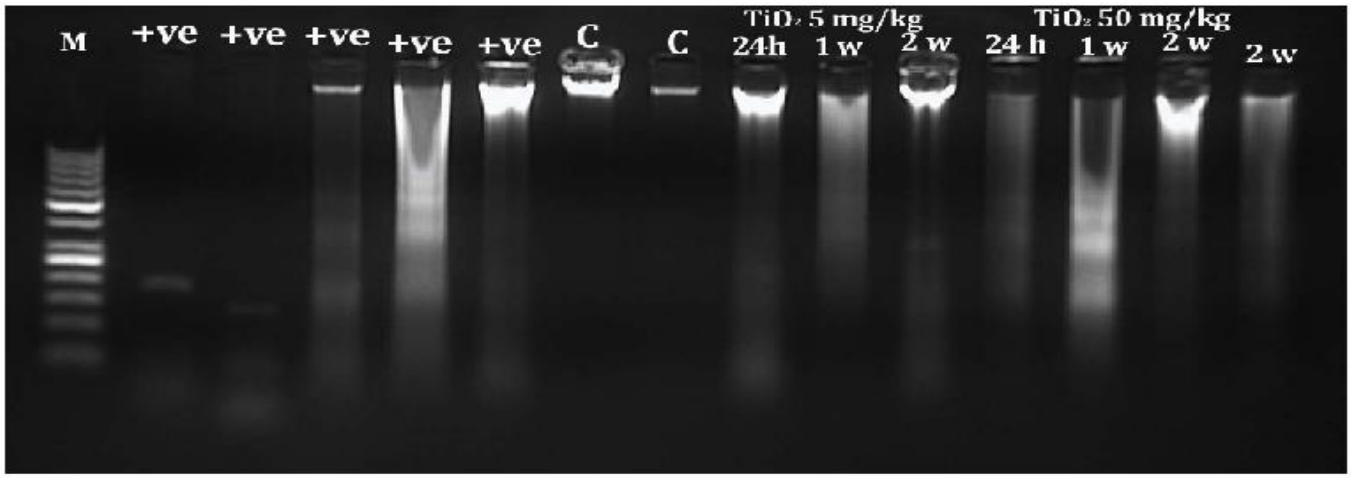

Fig. 1: Laddered DNA fragmentation of nano-TiO_2 treated groups compared with undamaged DNA from control group (C) and damaged DNA from the positive control group (+ve). M: marker

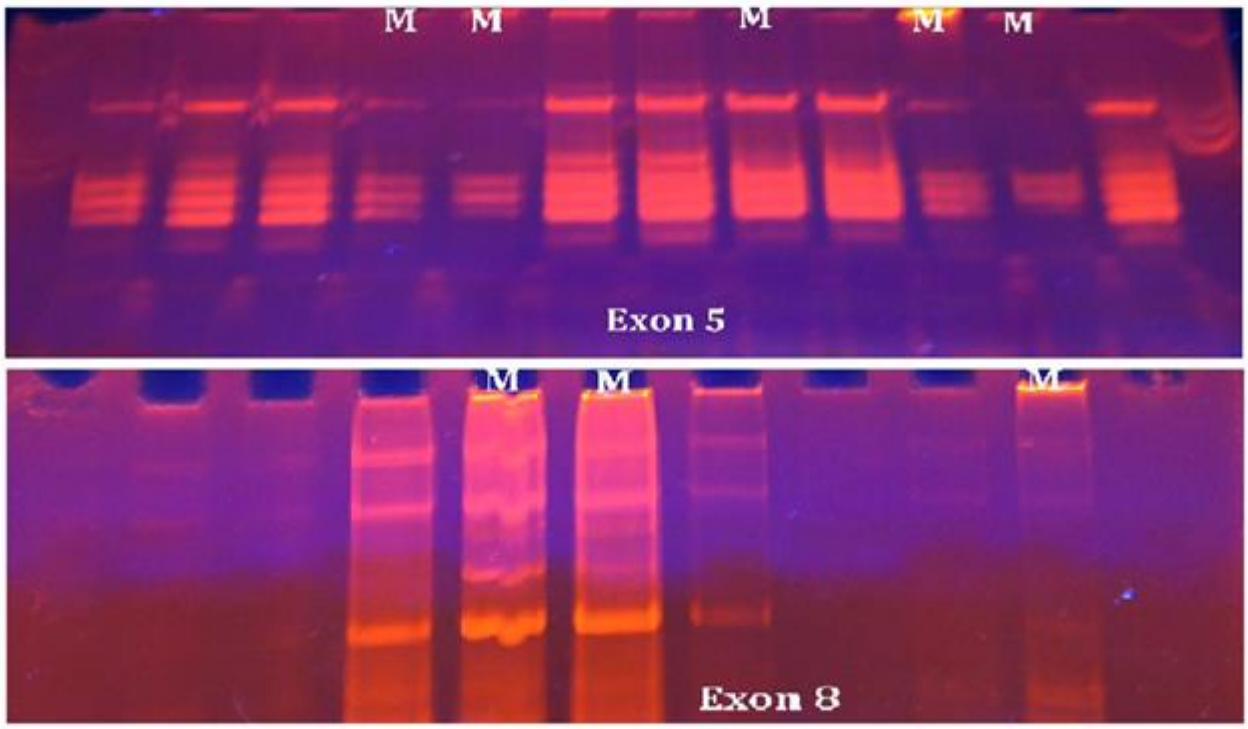

Fig. 2a: Representative photo for the observed mutations in p53 exon 5 & 8 regardless of dose and treatment M; mutant

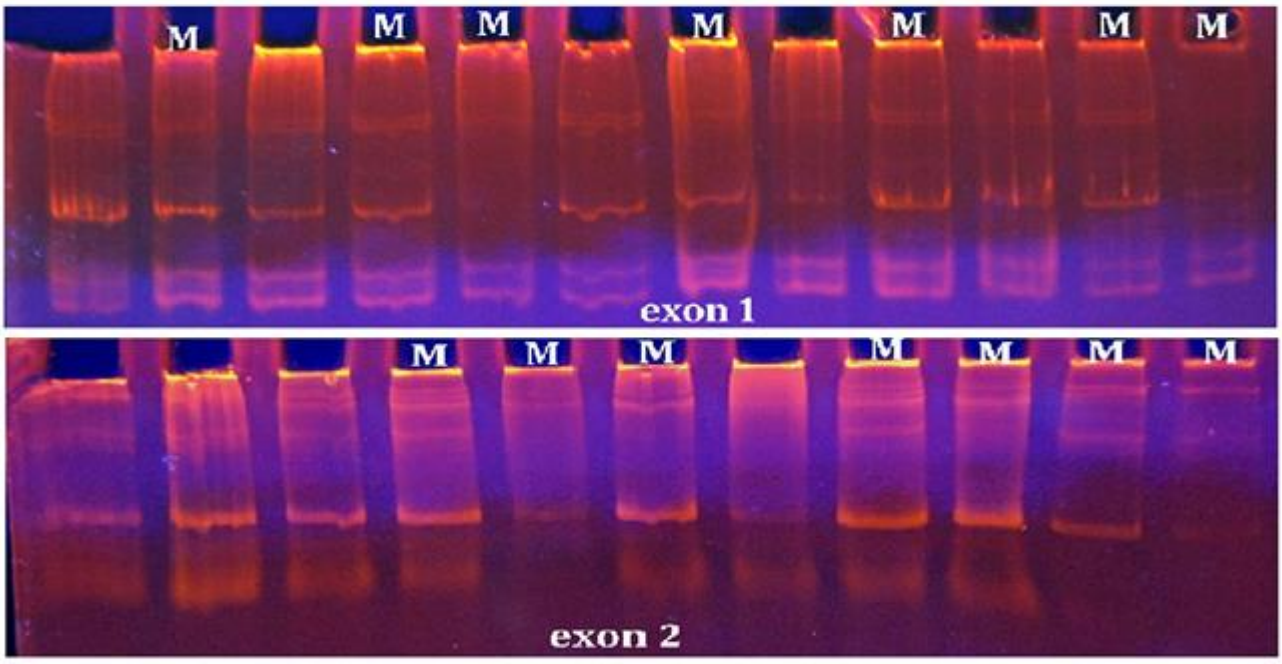

Fig. 2b: Representative photo for the observed mutations in H ras exons 1 & 2 regardless of dose and treatment; M: mutant

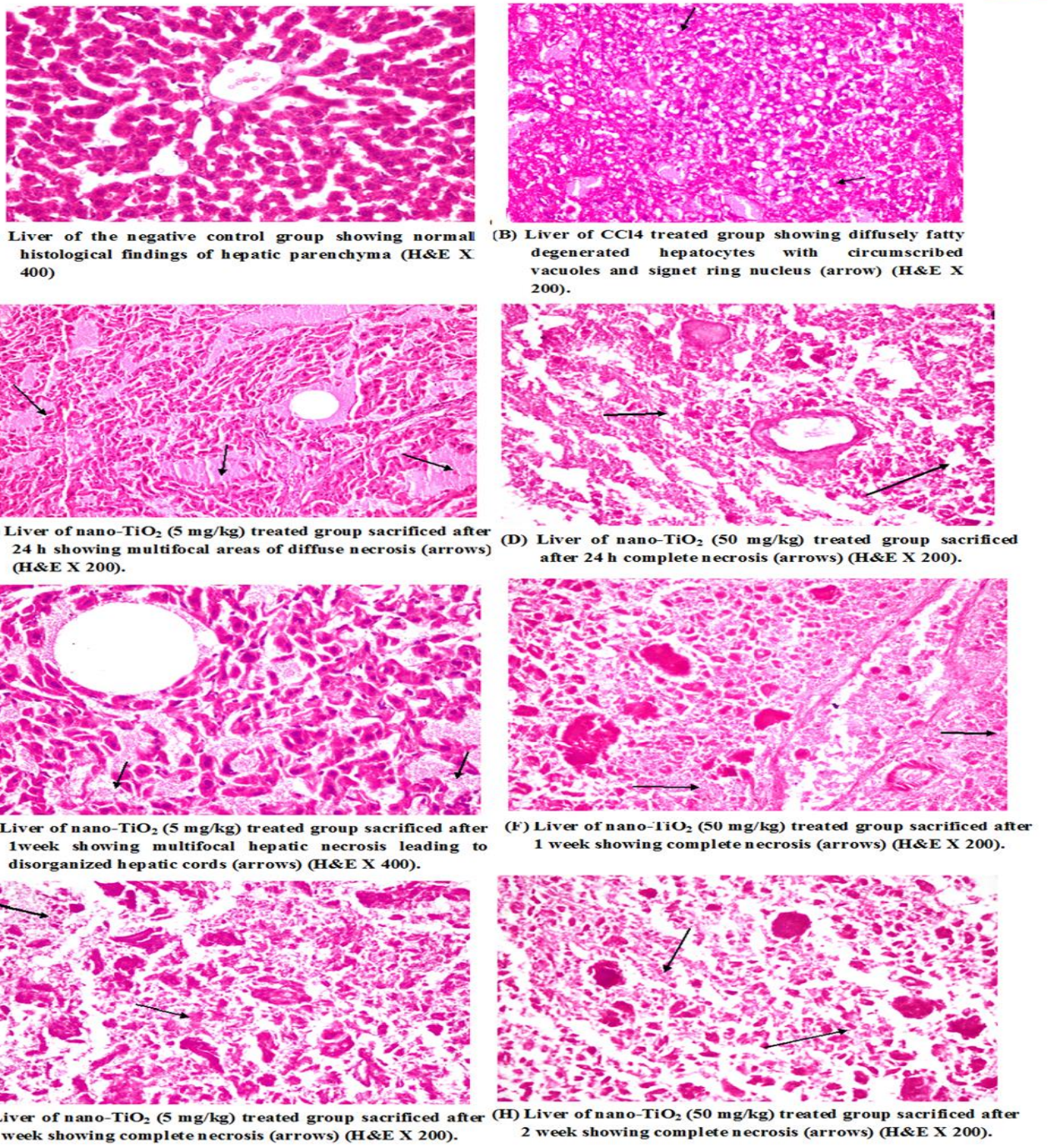

(A) Liver of the negative control group showing normal histological findings of hepatic parenchyma (H&E X 400)

(B) Liver of CCl4 treated group showing diffusely fatty degenerated hepatocytes with circumscribed vacuoles and signet ring nucleus (arrow) (H&E X 200).

(C) Liver of nano-TiO_2 (5 mg/kg) treated group sacrificed after 24 h showing multifocal areas of diffuse necrosis (arrows) (H&E X 200).

(D) Liver of nano-TiO_2 (50 mg/kg) treated group sacrificed after 24 h complete necrosis (arrows) (H&E X 200).

(E) Liver of nano-TiO_2 (5 mg/kg) treated group sacrificed after 1week showing multifocal hepatic necrosis leading to disorganized hepatic cords (arrows) (H&E X 400).

(F) Liver of nano-TiO_2 (50 mg/kg) treated group sacrificed after 1 week showing complete necrosis (arrows) (H&E X 200).

(G) Liver of nano-TiO_2 (5 mg/kg) treated group sacrificed after 2 week showing complete necrosis (arrows) (H&E X 200).

(H) Liver of nano-TiO_2 (50 mg/kg) treated group sacrificed after 2 week showing complete necrosis (arrows) (H&E X 200).

Fig. 3: Histopathological examination of liver tissue

Moreover, oral administration of nano-TiO_2 induced high mutation incidence in both exon 1 and 2 of H-ras gene as shown in table 3. In the case of exon 1: one out of four (25%) and three out of five (60%) mice were mutated in groups treated with nano-TiO2 two doses at 24 hours and two weeks respectively. While three (75%) and two (50%) out of four mice were mutated after one week of oral administration nano-TiO_2 at 5 and 50 mg/kg respectively. High mutation incidence was

also induced in H-ras exon 2 as shown in table 3 the frequencies of mutation were 50% and 80%, and were 25%, 50% and 60% 24 hours, one and two weeks after the last administration of 5 and 50 mg/kg of nano-titanium, respectively as shown in table 3. Representative examples for the observed mutation in H-ras exon 1 and 2 were shown in Fig. 2b.

Table 3: Incidence of mutation in p53 (exon 5 and 8) and H ras (exons 1 and 2) genes

Group	Treatment (mg/kg)	Duration	No of mutated mice/ total mice examined			
			P53		H ras	
			Exon 5	Exon 8	Exon 1	Exon 2
2	TiO_2 (5)	24 hour	0/4	2/4	1/4	2/4
		1 week	1/4	2/4	3/4	2/4
		2 weeks	3/5	3/5	3/5	4/5
3	TiO_2 (50)	24 hour	2/4	4/4	1/4	2/4
		1 week	1/4	4/4	2/4	1/4
		2 weeks	3/5	4/5	3/5	4/5

3.5 Histopathology

Histopathological examination evidenced the normal histological findings of hepatic parenchyma (H&E X 400) (Fig 3). On contrary, Liver tissue of positive control showed diffusely fatty degenerated hepatocytes with circumscribed vacuoles and signet ring nucleus like groups treated with nano-titanium two doses (5and 50 mg/kg) evidenced the tissue injuries by the presence of showing multifocal areas of diffuse necrosis leading to disorganized hepatic cords in 5 mg nano-titanium treated groups at 24 hours and one week. Moreover, complete necrosis was induced by higher nano-titanium dose (50 mg/kg) and by increasing sampling time to two weeks (H&E X200) (Fig. 3).

3.6 Oxidative stress markers

As shown in table 4 oral administration of TiO_2 nanoparticles statistically significantly increased the MDA level in liver tissues in a time-dependent manner compared with the negative control not only reached to the positive control

MDA level but also exceeded it after two weeks of oral administration of the highest nano-titanium dose. On the other hand, GSH concentration was lowered in mice subjected to nano-TiO_2 in a time dependent manner that reached to the positive control GSH level, unlike the negative control group which has the higher concentration of GSH.

4-Discussion

Extensive uses of nano-titanium increase the daily human exposure to it thereby increasing its risk. However, limited data are available on their bio-persistence and consequently cancer incidence in liver cells. Therefore, this study was designed to investigate the nano-titanium bio-persistence and its effect on hepatic cancer incidence in mice.

Table 4: The levels of MDA and GSH in the liver tissues of groups treated with nano-TiO_2 particles and the control groups

Group	Dose	Duration	MDA level (mmol/g. tissue)	GSH level (mmol/g tissue)
Negative Control	–	pooled	24.9 ±3.7	0.11±0.01
Positive Control	1 ml/kg	Pooled	$59.5\pm16.4^{a**}$	$0.05\pm0.01^{a***}$
Nano-TiO_2	5 mg/kg	24 h 1 week 2 week	$34.4\pm9.9^{b*}$ $39.4\pm11.1^{a*}$ $41.1\pm10.1^{a*}$	$0.07\pm0.01^{a**;b*}$ $0.06\pm0.01^{a*;b**}$ $0.06\pm0.03^{a*}$
Nano-TiO_2	5 mg/kg	24 h 1 week 2 week	$46.2\pm8.0^{a**}$ $50.19\pm12.4^{a**}$ $62.08\pm11.9^{a**}$	$0.065\pm0.01^{a***}$ $0.047\pm0.01^{a***}$ $0.053\pm0.02^{a**}$

Results are expressed as mean ± S.D. [a]: indicated statistically significant difference from the negative control group and [b]: indicated statistically significant difference from the positive control group at *: $p<0.05$, **: $p<0.01$ and ***: $p<0.001$

Daily human consumption of TiO_2 NPs through pastries, food, sweets, toothpaste, and even water (accumulated in which TiO_2 NPs as a result of wastes) results in individual ingestion of 10 mg of TiO_2 NPs from typical diet and even more if person's diet consisted of candies or highly

processed white foods e.g Candies ingestion results in person ingestion of 40 mg of nano-sized TiO_2 particles. Moreover, personal care products increase the human exposure to TiO_2 NPs as 1.5 g/day of sunscreen lead to human exposure to 6.3 mg of TiO_2 NPS/day that can be absorbed and distributed to various organs **(Weir, 2011; Weir et al., 2012).** Thus, the two selected and tested doses (5 and 50 mg / kg b.w) of TiO_2 NPs in our study represent the human exposure dose (5 mg/kg), as well as the highest dose (50 mg/kg) represents the accumulative dose of ingested low doses over a longer period.

First our results of comet assay evidenced the persistence of nano-TiO2 induced DNA damage by the observed persisted significant elevations in tail length, %DNA and tail moment with time during the experimental period in spite of stopping nano-titanium administration. This persisted nano-TiO_2 induced DNA damage was further amplified leading to apoptotic DNA damage of liver DNA as revealed by the fragmentized and smeared appearance of genomic DNA running on agarose until after two weeks of stopping treatment in a harmony with previous studies that showed that both single and double-strand-breaks have been shown to trigger apoptosis **(Lips and Kaina, 2001; Tounekti *et al*., 2001).** Several studies have been performed using the in vivo Comet assay in different tissues and evidenced DNA damage inductions by nano-TiO_2 particles **(Reeves *et al*., 2008; Trouiller *et al*., 2009; Mohamed, 2015).**

Oxidative stress is the suggested mechanism of nano-sized TiO_2 genotoxicity via its ability to increase the production of reactive oxygen species (ROS). Hydroxyl radicals, superoxide radical anions, hydrogen peroxide, and singlet oxygen are the ROS that formed by nano-TiO_2 (Chen *et al*., 2009). Hydroxyl radicals are the predominant radical species generated and play the major role in producing the genotoxic effects in terms of oxidative DNA damage **(Reeves *et al*., 2008)**. Moreover, nano-TiO_2- induced oxidative DNA damage has been proved by the determination of 8-hydroxy-deoxyguanosine(8OHdG), a good marker of oxidative DNA lesion **(Papageorgiou *et al*., 2007; Schins *et al*., 2002).**Thus, the observed nano-TiO_2-induced genotoxicity in the present study could be attributed to the accumulation of ROS generated by nano-titanium. In our study, the observed persisted significant time-dependent elevations in MDA level and decreases in GSH level confirmed ROS generation and disruption of the antioxidant defense system as a main mechanism for the observed persisted nano-titanium induced apoptotic DNA damage.

Progressive accumulation of DNA damage is a critical step in multistep chemical carcinogenesis in which at least two types of genes play an important role in neoplasia development:

proto-oncogenes and tumor suppressor genes which act in normal cells controlling proliferation. For example P53 and RAS family have been widely studied as damage of these genes are critical in the development of neoplasia and can be identified in different stages of the process. Therefore, in our study, we screened mutations in these two genes p53 and H-ras.

Results of SSCP analysis evidenced the mutation induction in p53 exons 5 & 8 by nano-TiO_2 particles in liver cells in a dose and time-dependent manner in spite of stopping the nano-titanium administration. Indeed, ROS generation and oxidative stress induction by nano-titanium results in increased mutation of the p53 gene and, moreover, apoptosis induction has been shown to be induced by increasing mutation inductions in p53 exons (5-8), independent of their type and location **(Slooten *et al*., 1999).** Therefore, the evidenced p53 mediated apoptosis in this study by the observed dose- and time-dependent high incidence in mutation of p53 exons (5 & 8) in nano-TiO2 treated groups could be attributed to p53 up-regulation since as previously reported the mutant p53 don't induce MDM-2 gene expression that resulting in its accumulation at very high concentrations and also worse mutant p53 protein itself can inhibit normal p53 **(Blagosklonny, 2002),** which is in line with the findings of **(French *et al*., 2001; Modur *et al*., 2002; Kang *et al*., 2008).**

Furthermore, the observed high incidence of H-ras mutation in groups treated with nano titanium increases the incidence of liver cancer as the 3 Ras genes in humans (HRas, Kras, and NRas) are the most common oncogenes in human cancer and Ras mutations permanently activate Ras and increase its expression for this reason, Ras inhibitors are being studied as a treatment for cancer, and other diseases with Ras overexpression **(Bitisch et al., 1993).**

Indeed, the observed gradual histopathological injuries in the liver tissues of nano-TiO_2 treated mice evidenced necrosis. First the appearance of vacuoles and diffused degenerated hepatocytes after 24 hours and one week of the last administration **(Johar *et al*., 2004; Alarifi *et al*., 2013; Faddah *et al*., 2013).** This subsequently leads to severed damage liver cells as shown by complete necrotic area and disorganized hepatic cords.

5-Conclusion

Oral administration of even the safe permitted exposure dose of nano titanium retained in the liver tissues thereby resulting in not only persisted but accumulative genotoxic and mutagenic effect that increases with time the incidence of not the only liver injury but also chemical induced hepatocellular carcinoma.

6-References

Alarifi, S., Ali, D., Al-Doaiss, A.A., Ali, B.A., Ahmed, M., Al-Khedhairy, A.A., (2013).

Histologic and apoptotic changes induced by titanium dioxide nanoparticles in the livers of rats. Int. J. Nanomed. 8, 3937e 3943.

Beutler., E., Duran O., and Kelly., B.,M., (1963). Improved method for the determination of blood glutathione, J Lab Clin Med. 1963,61,882.

Bitsch A, Röschlau H, Deubelbeiss C, Neumann HG, (1993). The structure and function of the H-RAS protooncogene are not altered in rat liver tumors initiated by 2acetylaminofluorene, 2-acetylaminophenanthrene and trans4-acetylaminostilbene. Toxicology Letters. 67(1-3), 173-86, 1993

Blagosklonny, MV, (2002). P53: An ubiquitous target of anticancer drugs. Int J Cancer. 98, 161-166

Chen, J., Dong, X., Zhaoa, J. and Tang, G., 2009.In vivo acute toxicity of titanium dioxide nanoparticles to mice after intraperitioneal injection. J. Appl. Toxicol. 29, 330–337

Faddah LM, Abdel Baky NA, Al-Rasheed NM and Al-Rasheed NM, (2013). Full Length Research Paper: Biochemical responses of nanosize titanium dioxide in the heart of rats following administration of idepenone and quercetin. African J. of Pharmacy and Pharmacology.7(38), 2639-265

French J.E., Lacks G.D., Trempus C., Dunnik J.K., Foley J., Mahler J., Tice R.R. and Tennant R.W, (2001). Loss of heterozygosity frequency at the Trp53 locus in p53-deficient (+/-) mouse tumors is carcinogen- and tissue-dependent. Carcinogenesis. 21(1), 99-106

Guichard, Y., Schmit, J., Darne, C., Gat´e, L., Goutet, M., Rousset, D., Rastoix, O., Wrobel, R., Witschger, O., Martin, A., et al., (2012). Cytotoxicity and genotoxicity of nanosized and microsized titanium dioxide and iron oxide particles in syrian hamster embryo cells. Ann. Occup. Hyg. 56, 631 – 644.

Gurr JR, Wang AS, Chen CH, Jan KY, (2005). Ultrafine titanium dioxide particles in the absence of photo activation can induce oxidative damage to human bronchial epithelial cells. Toxicology. 213, 66–73. PMID: 15970370

Gutierrez, M. I., Bhatia, K., Siwarski, D., Wolff, L., Magrath, I. T., Mushinski, J. F. and Huppi1, K., (1992). Infrequent p53 mutation in mouse tumors with deregulated myc. Cancer Res. 52, 1032–1035

Hu, C. W., Lia, M, Cui, Y. B., Li, D. S., Chen, J and Yang, L. Y., (2010). Toxicological effects of TiO2 and ZnO nanoparticles in

soilon earthworm Eisenia fetida. Soil Biol. Biochem. 42, 586–591.

Jeon, Y.-M., Park, S.-K. and Lee, M.-Y., (2011). Proteomic analysis of hepatotoxicity induced by titanium nanoparticles in mouse liver. J. Korean Soc. Appl. Biol. Chem. 54, 852–859.

Johar D, Roth JC, Bay GH, Walker JN, Kroczak TJ and Los M, (2004). Inflammatory response, reactive oxygen species, programmed (necrotic-like and apoptotic) cell death and cancer. *Rocz Akad Med Bialymst*.; 49:31–39.

Kang, S.J., Kim, B.M., Lee, Y.J. and Chung, H.W., (2008). Titanium dioxide nanoparticles trigger p53-mediated damage response in peripheral blood lymphocytes. Environ. Mol. Mutagen. 49, 399–405.

Lips and Kaina, (2001). DNA double-stranded breaks triggered apoptosis in p53 deficient fibroblast. Carcinogenesis. 22, 579-585

Long, T. C., Tajuba, J., Sama, P., Saleh, N., Swartz, C., Parker, J., Hester, S., Lowry, G. and Vand Veronesi, B., (2007). Nanosize titanium dioxide stimulates reactive oxygen species in brain microglia and damages neurons in vitro. Environ. Health Per- spect. 115, 1631–1637.

Masoud R, Bizouarn T, Trepout S, Wien F, Baciou L, Marco S, et al., (2014). Titanium Dioxide Nanoparticles Increase Superoxide Anion Production by Acting on NADPH Oxidase. PLoS ONE. 10(12), e0144829. doi:10.1371/journal.pone.0144829

Modur V, Nagarajan R, Evers BM and Milbrandt J, (2002). FOXO proteins regulate tumor necrosis factor-related apoptosis inducing ligand expression. Implications for PTEN mutation in prostate cancer. J Biol Chem. 277, 47928–47937.

Modur V, Nagarajan R, Evers BM and Milbrandt J., (2002). FOXO proteins regulate tumor necrosis factor-related apoptosis inducing ligand expression. Implications for PTEN mutation in prostate cancer. J Biol Chem. 277,47928–47937.

Mohamed, H.R.H., (2015). Estimation of TiO2 nanoparticle-induced genotoxicity persistence andpossible chronic gastritis-induction in mice. Food and Chemical Toxicology. 83, 76-83

Nakagawa, Y., Wakuri, S., Sakamoto, K. and Tanaka, N., (1997). The photogenotoxicity of titanium dioxide particles. Mutat. Res. 394, 125–132.

Ohkawa H, Ohishi W and Yagi K, (1979). Assay for lipid peroxides in animal tissues by thiobarbituric acid reaction. Anal Biochem. 95, 351-8

Papageorgiou, I., Brown, C., Schins, R., Singh, S., Newson, R., Davis,S.,Fisher,J., Ingham, E. and Case, C.P., (2007). The effect of nano- and micron-sized particles of cobalt-chromium al- loy on human fibroblasts in vitro. Biomaterials. 28, 2946–2958.

Reeves, J. F., Davies, S. J., Dodd, N. J. F. and Jha, A. N., (2008). Hy- droxyl radicals (OH) are associated with titanium dioxide (TiO2)nanoparticles-induced cytotoxicity and oxidative DNA damage in fish cells. Mutat. Res. 640, 113-122.

Schins, R. P., Duffin, R., Hohr, D., Knaapen, A. M., Shi, T., Weishaupt, C., Stone, V., Donaldson, K. and Borm, P. J., (2002). Surface modification of quartz inhibits toxicity, particle up- take, and oxidative DNA damage in human lung epithelial cells. Chem. Res. Toxicol. 15, 1166–1173.

Smulders, S., Luyts, K., Brabants, G., Landuyt, K. V., Kirschhock, C., Smolders, E., Golanski, L., Vanoirbeek, J., Hoet, P. H., (2014). Toxicity of nanoparticles embedded in paints compared with pristine nanoparticles in mice. Toxicological sciences: an official journal of the Society of Toxicology. 141(1), 132-40.

Tice, R. R., Agurell, E., Anderson, V., Burlinson, B., Hartmann, A., Kobayashi, H., Miyamae, Y., Rojas, E., Ryu, J. C. and Sasaki, Y. F., (2000). Single cell gel/comet assay: Guidelines for in vitro and in vivo genetic toxicology testing, Environ. Mol. Mutagen. 35, 206–221.

Tounekti O, Kenani A, Foray N, Orlowski S and Mir LM, (2001). The ratio of single- to double-strand DNA breaks and their absolute values determine cell death pathway. Br J Cancer; 84: 1272–1279

Trouiller, B., Relience, R., Westbrook, A., Solaimani, P. and Schiesll, R. H., (2009). Titanium dioxide nanoparticles induce DNA damage and genetic instability in vivo in mice. Cancer Res. 69, 8784–8789

Turrens J. F, (2003). Mitochondrial formation of reactive oxygen species. J. Physiol. 552(2), 335–344.

Watanabe H, Shimokado K, Asahara T, Dohi K and Niwa O, (1999). Analysis of the c-myc, K-ras and p53 Genes in Methylcholanthrene-induced Mouse Sarcomas. Jpn. J. Cancer Res. 90, 40–47

Weir A.A, (2011). TiO2 Nanomaterials: Human Exposure and Environmental Release. M.Sc thesis. Arizona State University

Weir, A., Westerhoff P, Fabricius L, Hristovski K, von Goetz N, (2012). Titanium dioxide nanoparticles in food and personal care products. ***Environ Sci Technol***. 46, 2242–2250